

# High-Dimensional Causal Discovery: Learning from Inverse Covariance via Independence-based Decomposition

Shuyu Dong<sup>\*</sup>, Kento Uemura<sup>†</sup>, Akito Fujii<sup>†</sup>, Shuang Chang<sup>†</sup>, Yusuke Koyanagi<sup>†</sup>,  
Koji Maruhashi<sup>†</sup>, and Michèle Sebag<sup>\*</sup>

<sup>\*</sup>LISN, INRIA, Université Paris-Saclay, France  
first.last@inria.fr, first.last@lri.fr  
<sup>†</sup>Fujitsu Laboratories Ltd., Japan  
first.last@fujitsu.com

November 23, 2022

## Abstract

Inferring causal relationships from observational data is a fundamental yet highly complex problem when the number of variables is large. Recent advances have made much progress in learning causal structure models (SEMs) but still face challenges in scalability. This paper aims to efficiently discover causal DAGs from high-dimensional data. We investigate a way of recovering causal DAGs from inverse covariance estimators of the observational data. The proposed algorithm, called ICID (inverse covariance estimation and *independence-based* decomposition), searches for a decomposition of the inverse covariance matrix that preserves its nonzero patterns. This algorithm benefits from properties of positive definite matrices supported on *chordal* graphs and the preservation of nonzero patterns in their Cholesky decomposition; we find exact mirroring between the support-preserving property and the independence-preserving property of our decomposition method, which explains its effectiveness in identifying causal structures from the data distribution. We show that the proposed algorithm recovers causal DAGs with a complexity of  $O(d^2)$  in the context of sparse SEMs. The advantageously low complexity is reflected by good scalability of our algorithm in thorough experiments and comparisons with state-of-the-art algorithms.

## 1 Introduction

Discovering causal relations from observational data emerges as an important problem for artificial intelligence [Pea00, PJS17] with fundamental and practical motivations. One notable reason is that causal models support modes of reasoning, e.g., counterfactual reasoning and algorithmic recourse [TKL<sup>+</sup>21], that are otherwise out of reach by

correlation-based machine learning, as recent developments [PBM16, ABGLP19, SG21] show how causal structure learning can contribute to mainstream machine learning.

The learning of causal structures from data is, however, NP-hard [Chi96]. A major challenge is that the search space of causal structures—which corresponds to the space of all possible directed acyclic graphs (DAGs)—grows quickly in dimension, with a superexponential rate, with respect to the number  $d$  of variables in question. Concretely, one needs to ensure that the causal structure candidate stays in the space of DAGs and at the same time, keep the search within an affordable amount of time and computation cost. To overcome the first difficulty, PC [KB07] and LiNGAM [SHHK06, SIS<sup>+</sup>11] use independence-based constraints, e.g., conditional independence tests, to ensure the search within the space of DAGs; and for a reduced computational burden, local search strategies such as GES [Chi02] and the limited tree-width search of [LB14] (see Section 2.2), are proposed. Further progresses are made by recent methods that try to address both difficulties at the same time. [ZARX18] proposed an optimization approach, called NOTEARS, that searches a candidate DAG in the relaxed, continuous space of all weighted adjacency matrices of DAGs, which can be [ZARX18] identified with a fixed level set of the exponential trace  $h(B) := \text{tr}(\exp(B \odot B))$ . Subsequently, various recent work [KGG<sup>+</sup>18, YCGY19, ZDA<sup>+</sup>20, FZZ<sup>+</sup>20] propose to address causal structure learning in different ways within the constrained optimization approach using the exponential trace function. Other lines of recent work address causal structure learning based on statistical inference such as inverse covariance estimation [LB14, GH18, NZZZ21], maximum-likelihood estimation (MLE) [NGZ20], Bayesian inference [VHPK20, CGE21] and deep generative models [DGE<sup>+</sup>22]. The difficulties of scaling causal learning methods to high-dimensional data still persist. For continuous optimization methods (e.g., NOTEARS), the time complexity is  $O(d^3)$  owing to the gradient computations of  $h$ ; Bayesian inference methods [VHPK20, CGE21] and constraint-based sequential methods (e.g., LiNGAM) achieve good learning precisions at costs even higher than  $O(d^3)$ .

In this paper, we are interested in learning large causal structures. We propose a framework named ICID (Inverse Covariance estimation and Independence-based Decomposition) for making causal discovery from the inverse covariance matrix of a multivariate system. It is known that, under the linear Structure Equation Model (SEM), the inverse covariance matrix  $\Theta$  of the system is related to the adjacency matrix  $B$  of the causal DAG by a matrix equation in the form of  $\Theta \propto (I - B)(I - B)^T$ . Previous efforts [LB14, GH18] that extract causal information from inverse covariance are limited to small- and mid-sized graphs due to the complexity of (local) DAG enumeration or to the sequential nature of the causal recovery method. Interestingly, we show that it is possible to recover the causal DAG by computing a specific, *support preserving* decomposition of the inverse covariance matrix. This theoretical confirmation, based on properties of *chordal* graphs regarding the Cholesky decomposition of their adjacency matrices, explains the effectiveness of matrix decomposition within our algorithm. Our contributions are:

- We establish a relation between causal DAG recovery from inverse covariance

estimators and graph characterizations of sparse matrix decomposition. This result justifies the use of our decomposition approach, which has a mirroring with Cholesky decomposition of symmetric positive definite matrices, for recovering causal DAGs.

- For a broader applicability, we enhance the decomposition method with a recent low-complexity method for computing weighted adjacency matrices of proximal DAGs. We show that the proposed method, unlike previous methods, has two distinct steps—the first being a statistical inference problem (inverse covariance estimation) and the second a pure geometrical and matrix algebraic problem—that both enjoy an  $O(d^2)$  complexity, which is significantly lower than previous methods. This gives new understandings on causal structure learning in relation with undirected graphical models.
- We demonstrate, through extensive experiments, that the proposed method gains significantly in time efficiency for learning large causal structures from data.

## 2 Background and related work

### 2.1 Notation

A graph on  $d$  nodes is defined and denoted as a pair  $\mathcal{G} = (\mathcal{V}, \mathcal{E})$ , where  $|\mathcal{V}| = d$  and  $\mathcal{E} \subset \mathcal{V} \times \mathcal{V}$ . By default, any directed graph is simply referred to as a graph. The adjacency matrix of a graph  $\mathcal{G}$ , denoted as  $\mathbb{A}(\mathcal{G})$ , is defined as the matrix such that  $[\mathbb{A}(\mathcal{G})]_{ij} = 1$  if  $(i, j) \in \mathcal{E}$  and 0 otherwise. Let  $B_{\mathcal{G}} := B \in \mathbb{R}^{d \times d}$  be any *weighted* adjacency matrix of a graph  $\mathcal{G}$  on  $d$  nodes, then by definition, the adjacency matrix  $\mathbb{A}(\mathcal{G})$  indicates the nonzeros of  $B$ . Conversely, for any  $B \in \mathbb{R}^{d \times d}$ , the (0-1) matrix that indicates all nonzeros of  $B$  by 1 (and all zeros of  $B$  by 0) is exactly the adjacency matrix of the *support graph* of  $B$ , defined as  $\text{supp}(B) := \{(i, j) : B_{ij} \neq 0\}$ . We call matrix  $B$  a *DAG matrix* if  $\text{supp}(B)$  is a DAG, and denote the set of DAG matrices as  $\mathcal{D}_{d \times d} := \{B \in \mathbb{R}^{d \times d} : \text{supp}(B) \text{ is a DAG}\}$ . Given a DAG  $\mathcal{G}$ , the moralization of  $\mathcal{G}$  is an operation of producing an undirected graph  $\mathcal{M}(\mathcal{G})$  by fully connecting all nodes within each parent set in  $\mathcal{G}$  (and symmetrizing the directed edges to undirected ones).

The number of nonzeros of  $B$  is denoted as  $\|B\|_0 = \text{nnz}(B)$  indifferently. The set of  $d \times d$  symmetric positive definite matrices is denoted by  $\mathcal{S}_{++}^d$  and the positive definiteness of a symmetric matrix  $\Theta$  is also expressed as  $\Theta \succ 0$ .

### 2.2 Structural Equation Models

Structural equation models (SEMs) are introduced as a graphical model for probabilistic reasoning and causal analysis. A SEM defined on a set of random variables  $\mathbf{X} = (X_1, \dots, X_d)$  is associated with a directed acyclic graph (DAG)  $\mathcal{G}$  with  $d$  nodes and a joint distribution  $P(\mathbf{X})$  satisfying the Markov condition with respect to the DAG  $\mathcal{G}$ , that is,  $P(x) = \prod_{i=1}^d P(x_i | x_{\text{PA}_i^{\mathcal{G}}})$ , where  $\text{PA}_i^{\mathcal{G}}$  is the set of parent nodes of  $X_i$  in  $\mathcal{G}$ .

Linear SEMs consist of a basic and important subset of SEMs, for which the (causal) interdependences among the variables are expressed as

$$\mathbf{X} = B^T \mathbf{X} + \mathbf{E}, \quad (1)$$

where  $B$  is a (weighted) adjacency matrix of the DAG  $\mathcal{G}$ , and  $\mathbf{E}$  is random variable modeling i.i.d. additive noises along the  $d$  dimensions.

A SEM (1) is described from its causal graph matrix  $B^* \in \mathcal{D}_{d \times d}$  and  $\Omega$  is a positive diagonal matrix of noise variances. It follows from (1) that the covariance of  $\mathbf{X}$  is  $\Sigma = (I - B)^{-T} \Omega (I - B)^{-1}$ . Consequently, the inverse covariance matrix  $\Theta$  of the system, also called the precision matrix, can be expressed as

$$\Theta = (I - B) \Omega^{-1} (I - B)^T. \quad (2)$$

The following lemma and theorem in [LB14] give a refined description of how the inverse covariance matrix  $\Theta$  is related to the causal graph matrix  $B$ .

**Lemma 1** ([LB14, Lemma 1]). *Suppose that (i) the covariance matrix  $\mathbf{E}$  of noises is diagonal  $\Omega := \text{diag}(\sigma_1^2, \dots, \sigma_d^2)$  for some  $\sigma_i > 0$  and (ii) the graph node ordering (with (1)) is such that matrix  $B$  is strictly upper triangular. Then the entries of  $\Theta$  are given by*

$$\Theta_{jk} = -\sigma_k^{-2} B_{jk} + \sum_{\ell > k} \sigma_\ell^{-2} B_{j\ell} B_{k\ell}, \quad \forall j < k, \quad (3)$$

$$\Theta_{jj} = \sigma_j^{-2} + \sum_{\ell > j} \sigma_\ell^{-2} B_{j\ell}^2, \quad \forall j. \quad (4)$$

In particular, (3) gives further clue to how the nonzero patterns of  $\Theta$  and  $B$  are related.

**Theorem 2** ([LB14, Theorem 2]). *Suppose  $X$  is generated from the linear SEM. Then,  $\Theta$  reflects the graph structure of the moralization  $\mathcal{M}(\mathcal{G})$ , i.e., for  $j \neq k$ , we have  $\Theta_{jk} = 0$  if  $(j, k)$  is not an edge in  $\mathcal{M}(\mathcal{G})$ .*

The theorem above has an important implication for causal inference since it tells how causal relations determine the correlations (nonzeros) between variables of a linear SEM system.

### 3 Independence-based Decomposition: motivation and main result

Based on findings about how inverse covariance is related to the hidden causal structure, we consider the problem of causal structure learning in two consecutive steps: first, inverse covariance estimation, which is a statistical inference problem and second, recovering a causal structure matrix  $B$  by *solving* the matrix equation (2) relating  $B$

with  $\Theta$ . The distinction between the statistical and geometrical parts of the problem is meaningful in the sense that it enables us to identify the difficulties of causal structure learning: all difficulties related to statistical inference in high dimensions are supposed to be entirely reflected in inverse covariance estimation, and the difficulty of searching in the nonconvex space DAGs is reflected in the search of a solution to the matrix equation (2).

The faithfulness of inverse covariance estimation in high dimensions is a well studied subject in statistics [WJ06, WLR06, BEGd08, FHT07]. Graphical Lasso [FHT07], for example, is a MLE method for estimating the inverse covariance in high dimensions. Therefore, we focus on the question of solving the matrix equation (2) in the context of causal structure learning and linear SEMs.

### 3.1 Sparse graphs and causal structure characterizations

Given an inverse covariance estimator  $\Theta \in \mathcal{S}_{++}^d$ , a simple decomposition  $\Theta = (I - B)(I - B)^T$ —according to (2)—is generally not able to recover the true adjacency matrix  $B^*$  of the linear SEM (1) faithfully. This is because the matrix decomposition of the form  $\Theta = AA^T$  admits multiple (in fact,  $d!$ ) solutions  $(A', Q)$  such that  $\Theta = A'QQ^T A'^T$ , where  $Q$  is a permutation matrix. A key question is *what additional constraints can be imposed to alleviate the ambiguity with different possible permutations*.

As shown in Lemma 1–Theorem 2 [LB14], the support of  $\Theta$  is a rather faithful superstructure of the true causal graph. Furthermore, we show next that the support constraint  $\text{supp}(B) \subset \text{supp}(\Theta)$  helps determining the true causal graph in the above mentioned matrix decomposition process.

Given an undirected graph  $\mathcal{G} = (\mathcal{V}, \mathcal{E})$  endowed with a node ordering  $\sigma$ , the following sets are considered:

$$\mathcal{S}_{\mathcal{G}, \sigma} = \{\Theta \in \mathcal{S}_{++}^d : \Theta_{ij} = 0 \text{ for } (\sigma^{-1}(i), \sigma^{-1}(j)) \notin \mathcal{E}\}, \quad (5)$$

$$\mathcal{L}_{\mathcal{G}, \sigma} = \{L \in \mathbb{R}^{d \times d} : L_{ii} = 1, L_{ij} = 0 \text{ for } i < j \text{ or } (\sigma^{-1}(i), \sigma^{-1}(j)) \notin \mathcal{E}\}. \quad (6)$$

The sets  $\mathcal{S}_{\mathcal{G}, \sigma}$  and  $\mathcal{L}_{\mathcal{G}, \sigma}$  are involved in the concept of  $\mathcal{G}$  being a graph that *factors without fill*: a sparsity pattern  $\mathcal{E}(G)$  is said to *factor without fill* if every matrix  $S$  with sparsity pattern  $\mathcal{E}(G)$  (meaning  $S \in \mathcal{S}_{\mathcal{G}, \sigma}$  for some  $\sigma$ ) can be factored into  $LDL^T$  such that  $L + L^T$  also has sparsity pattern  $\mathcal{E}(G)$ .

The following lemma [PPS89] describes the type of support graphs on which positive definite matrices can *factor without fill*. The notion of *chordal* graphs is used: an undirected graph is chordal if every cycle of length greater than three has a chord, i.e., a “shortcut” that triangulates the cycle.

**Lemma 3** ([PPS89]). *Let  $\mathcal{G} = (\mathcal{V}, \mathcal{E})$  be a chordal graph,  $\sigma$  an ordering of  $\mathcal{V}$  which corresponds to a perfect elimination ordering of  $\mathcal{G}$ . Then it holds that  $\Sigma \in \mathcal{S}_{\mathcal{G}, \sigma}$  (5) if and only if  $L \in \mathcal{L}_{\mathcal{G}, \sigma}$  (6), where  $L$  is the Cholesky factor of  $\Sigma$  such that  $\Sigma = LDL^T$ .*

The lemma above means that, for any positive definite matrix  $\Sigma$  supported on a chordal graph  $\mathcal{G}$ , the Cholesky decomposition of  $\Sigma$ —up to a certain node ordering—preserves the nonzeros pattern of  $\Sigma$  in the factor matrix  $L$ . The preservation of nonzeros

also holds for any  $\Sigma = LDL^T$  where  $L$  is a lower triangular matrix with support included in  $\mathcal{G}$ .

Similarly, [FG65] showed that if a sparsity pattern  $E$  is chordal, then there exists a permutation matrix  $Q$  such that  $\Sigma = QEQ^T$  factors without fill; see [FZS18, 2.B].

Consequently, we have the following theorem.

**Theorem 4.** *Let  $\Theta \in \mathcal{S}_{++}^d$  be a positive definite matrix whose support graph  $\text{supp}(\Theta)$  is chordal. Then the constrained decomposition problem:*

$$\begin{aligned} \min_{A \in \mathbb{R}^{d \times d}} \quad & \frac{1}{2} \|AA^T - \Theta\|_{\mathbb{F}}^2 \\ \text{subject to} \quad & \text{supp}(A) \subset \text{supp}(\Theta), \end{aligned} \tag{7}$$

*admits a minimizer  $A'$  such that  $A'$  represents a DAG and  $A'A'^T = \Theta$ .*

*Proof.* Since  $\mathcal{G} = \text{supp}(\Theta)$  is chordal,  $\mathcal{G}$  has a perfect elimination ordering that we denote as  $\sigma_0$ . Based on Lemma 3,  $\mathcal{G}$  being chordal implies that, for a certain node permutation  $\sigma$  (corresponding to the permutation matrix  $P_\sigma$ ), the positive definite matrix  $\tilde{\Theta} := P_\sigma \Theta P_\sigma^T$  belongs to  $\mathcal{S}_{\mathcal{G}, \sigma_0}$  (5) and that the (lower-triangular) Cholesky factor matrix  $\tilde{L}$  of  $\tilde{\Theta}$  (such that  $\tilde{L}\tilde{D}\tilde{L}^T = \tilde{\Theta}$  for a diagonal matrix  $\tilde{D}$ ) satisfies  $\tilde{L} \in \mathcal{L}_{\mathcal{G}, \sigma_0}$  (6). As a consequence, the matrices  $(A, D)$  which are  $\sigma$ -similar to  $(\tilde{L}, \tilde{D})$ , i.e.,  $A := P_\sigma^T \tilde{L} P_\sigma$  and  $D := P_\sigma^T \tilde{D} P_\sigma$  satisfy:

$$ADA^T = P_\sigma^T \tilde{L} \tilde{D} \tilde{L}^T P_\sigma = P_\sigma^T \tilde{\Theta} P_\sigma = \Theta,$$

which means that  $A' = A\sqrt{D}$  satisfies  $A'A'^T = \Theta$ . Moreover, it holds that  $\text{supp}(A') \subset \text{supp}(\Theta)$  because (i) the two support graphs are identical to  $\text{supp}(\tilde{L})$  and  $\text{supp}(\tilde{\Theta})$ , respectively, up to the node permutation  $\sigma$  and (ii)  $\text{supp}(\tilde{L}) \subset \text{supp}(\tilde{\Theta})$  by Lemma 3. Therefore  $A'$  is a global minimum of (7). Note that  $A'$  is  $\sigma$ -similar to  $\tilde{L}D'$  (with diagonal  $D' = P_\sigma \sqrt{D} P_\sigma^T$ ), which is a strict triangular matrix. Hence  $A'$  represents a DAG.  $\square$

The Cholesky decomposition in Lemma 3 is related to the decomposition (7) in the sense that it coincides with (7) if the true DAG adjacency matrix  $B^*$  in the linear SEM is strictly triangular, for a certain node ordering  $\sigma$ ; this condition is as strong (and difficult) as learning the causal structure itself. Instead, Theorem 4 above confirms that, without requiring explicitly the desired permutation  $P_\sigma$  and Cholesky decomposition, it suffices to compute the support-preserving decomposition of  $\Theta$  in the form of (7).

In view of Theorem 2, the true inverse covariance  $\Theta^*$  corresponds to the moralization  $\mathcal{M}(B^*)$ , which is slightly weaker than being chordal (if it happens to be not chordal). An estimator of  $\Theta^*$  will eventually become chordal if it has some additional edges (or *fills*) compared to the moralization  $\mathcal{M}(B^*)$ , preferably to the extent that the number of fills is as few as possible. In all cases (whether  $\text{supp}(\Theta)$  is chordal or not), solution of (7) can be used as a starting point around which DAGs are searched, as we will explain next in Section 4.

## 4 ICID: sparse matrix decomposition and algorithms

Based on the main result in Section 3, we propose to recover a DAG through (7) with a slightly enhanced constraint, given an inverse covariance estimator  $\Theta$ :

$$\begin{aligned} \min_{B \in \mathbb{R}^{d \times d}} \quad & \frac{1}{2} \|\Theta - \phi(B)\|_{\mathbb{F}}^2 + \lambda'_1 \ell_1(B) \\ \text{subject to} \quad & h(B) = 0, \quad \text{supp}(B) \subset \text{supp}(\Theta), \end{aligned} \quad (8)$$

where functions  $\phi$  and  $h$  are:

$$\phi(B) = (I - B)(I - B)^{\text{T}}, \quad h(B) = \text{tr}(\exp(B \odot B)) - d. \quad (9)$$

The definition of  $\phi(B)$  above is motivated by the relation (2) under the linear SEM with equivariance noises ( $\Omega = \sigma_N I$ ). The zero level-set of  $h$  (9) is shown to be an exact characterization of weighted adjacency matrices of DAGs [ZARX18]. Hence, the additional constraint with  $h(B)$  on top of (7) ensures the search of solutions in the set of DAGs; it can also be seen as an enhancement when  $\text{supp}(\Theta)$  is not chordal.

The support-preserving condition ( $\text{supp}(B) \subset \text{supp}(\Theta)$ ) in (7) and (8) mirrors the relations between the causal structure and conditional independences in the context of causal discovery. Therefore, we refer to problem (8) as *independence-based* decomposition. Algorithm 1 (ICID) describes a straightforward application of decomposition (8) for causal discovery from observational data.

---

**Algorithm 1** ICID for estimating DAGs from data

---

**Input:** Observational data  $X \in \mathbb{R}^{n \times d}$  from a linear SEM, parameters  $\lambda_1, \lambda'_1$

**Output:** DAG  $\hat{B}$  of the linear SEM

- 1: Get an inverse covariance matrix (using e.g., GraphicalLasso, QUIC):

$$\hat{\Theta} = \text{Inverse Covariance Estimation}(X, \lambda_1).$$

- 2: Solve the independence-based decomposition (8): # see Algorithm 2

$$\begin{aligned} \hat{B} = \arg \min_{B \in \mathbb{R}^{d \times d}} \quad & \frac{1}{2} \|\hat{\Theta} - \phi(B)\|_{\mathbb{F}}^2 + \lambda'_1 \ell_1(B) \\ \text{subject to} \quad & h(B) = 0, \quad \text{supp}(B) \subset \text{supp}(\Theta). \end{aligned}$$

---

The estimation of inverse covariance, in line 1 of Algorithm 1 is subject of extensive studies in the literature of graphical models and optimization [WJ06, WLR06, BEGd08, FHT07]. One notable formulation is the GraphicalLasso formulation [FHT07]:

$$\hat{\Theta} = \arg \min_{\Theta \succ 0} \text{tr}(C\Theta) - \log \det \Theta + \lambda_1 \ell_1(\Theta), \quad (10)$$

where  $C$  is the empirical covariance of  $\mathbf{X}$  and  $\lambda_1 \ell_1(\cdot)$  is the  $\ell_1$  norm-based penalty function of the vectorization of  $\Theta$ .

We solve (8) using an adaptation of the alternating minimization algorithm (AMA). We address the equality constraint  $h(B) = 0$  via the standard Lagrangian method and then split the minimization of  $\ell_2(B)$  and  $h(B)$  in two alternating subproblems:

$$B_{t+1} = \arg \min_{\text{supp}(B) \subset \text{supp}(\Theta)} \left\{ \frac{1}{2} \|\Theta - \phi(B)\|_{\text{F}}^2 + \lambda'_1 \ell_1(B) + \gamma_1 \|c_0 B - \tilde{B}_t\|_{\text{F}}^2 \right\} \quad (11)$$

$$\tilde{B}_{t+1} = \arg \min_{B \in \mathbb{R}^{d \times d}} h(B) + \frac{\gamma_2}{2} \|B - B_{t+1}\|_{\text{F}}^2 \quad (12)$$

Notice that the independence-based constraint of (11) restricts its search space to the subspace of all subgraphs of  $\text{supp}(\Theta)$ , and the objective function of (11) is convex. Hence, we consider an approximation of (11) via the following interpolation:

$$\hat{B}_{t+1} := \tau \tilde{B}_t + (1 - \tau) B_0,$$

where  $B_0$  is solution to the decomposition (13), which is an instance of (7) with  $\ell_1$ -penalty. To justify this interpolation, we notice that the line segment  $[B_0; \tilde{B}_t]$  is a subset of the feasible set  $\{B : \text{supp}(B) \subset \text{supp}(\Theta)\}$ , i.e., all points (matrices) on this segment are feasible. Hence,  $\hat{B}_{t+1}$  is a more optimal matrix than  $B_0$  and  $\tilde{B}_t$  regarding the objective of (11).

The detailed procedure is given in Algorithm 2.

---

**Algorithm 2** Independence-based Decomposition from inverse covariance

---

**Input:** Inverse covariance matrix  $\Theta \in \mathbb{R}^{d \times d}$

- 1: Initialize:  $\gamma_1 = 0, \gamma_2 = 1$ .
- 2: independence-based decomposition:

$$B_0 = \arg \min_{\text{supp}(B) \subset \text{supp}(\Theta)} \frac{1}{2} \|\Theta - \phi(B)\|_{\text{F}}^2 + \lambda'_1 \ell_1(B) \quad (13)$$

- 3: **for**  $t = 1, \dots$ , **do**
- 4:   **if** stopping criteria( $B_t, \tilde{B}_t$ ) attained **then**
- 5:     return  $B_t$
- 6:   **end if**
- 7:   Compute proximal mappings:

$$B_{t+1} = (1 - \rho) B_0 + \rho \tilde{B}_t \quad (14)$$

$$\tilde{B}_{t+1} = \text{prox}_{\gamma_2 h}(c_0 B_{t+1}) \quad (15)$$

- 8:   Increment  $\gamma_1, \gamma_2$ .
  - 9: **end for**
- 

We compute the initial decomposition (13) by using the FISTA [BT09].



*Remark 5* (Oracle ICID). Since Algorithm 2 takes as input a given precision matrix, we also use it independently from the global Algorithm 1, for recovering causal DAGs from the oracle precision matrix  $\Theta := \phi(B^*)$  of linear SEMs. Hence, we refer to Algorithm 2 as the oracle ICID method, labeled as  $\mathcal{O}$ -ICID in the experimental benchmarks.  $\square$

**Computation of proximal DAGs.** For subproblem (12) of the AMA, we use the low-rank algorithm of [DS22] for computing the proximal mapping of the DAGness function  $h$ .

#### 4.1 Computational properties and complexity

**Proposition 6.** *In the equivariance case where  $\Omega = \sigma_N I$ , the gradient of  $\ell_2(B) := \frac{1}{2} \|\Theta - \phi(B)\|_{\mathbb{F}}^2$  is*

$$\nabla \ell_2(B) = 2\sigma_N^{-1}(\Theta - \phi(B))(I - B).$$

*Proof.* Denote  $\lambda := \sigma_N^{-1}$  and  $\phi(B) := (I - B)(I - B)^T$ , for brevity. Then  $\ell_2(B) = \frac{1}{2} \|\lambda\phi(B) - \Theta\|_{\mathbb{F}}^2$ , and its differential at  $B$  is as follows, for any  $\xi \in \mathbb{R}^{d \times d}$ ,

$$D\ell_2(B)[\xi] = \langle \lambda\phi(B) - \Theta, \lambda D\phi(B)[\xi] \rangle. \quad (16)$$

Given that  $D\phi(B)[\xi] = (B - I)\xi^T + \xi(B - I)^T$ , and that  $\lambda\phi(B) - \Theta$  is symmetric, it follows from (16) that

$$D\ell_2(B)[\xi] = 2\lambda \langle \lambda\phi(B) - \Theta, \xi(B - I)^T \rangle = 2\lambda \langle (\lambda\phi(B) - \Theta)(B - I), \xi \rangle.$$

By identification, the gradient of  $\ell_2(B)$  is  $\nabla \ell_2(B) = 2\lambda(\Theta - \lambda\phi(B))(I - B)$ .  $\square$

The computational cost of ICID (Algorithm 1) is  $O(d^2)$  for learning sparse graphs. More precisely, the complexity of

- inverse covariance estimation is  $Cd^2$ , where  $C$  is an upper bound of the number of iterations for GraphicalLasso, and the sparse matrix multiplications therein are bound by  $d^2$ .
- the sparse matrix decomposition (8) is bounded by  $d^2$ , for the same reason above.
- the proximal mapping computation in (15) is also  $O(d^2)$ , benefiting from the low-rank method of [DS22].

#### 4.2 Connections with related work

[LB14, GH18] extract causal information by precise relations between the inverse covariance matrix—under the linear SEM—and the causal structure  $B^*$ . Moreover, [GH18] gives a more relaxed identifiability condition than the faithfulness assumption in [NGZ20]. However, the method in [LB14] uses an enumeration strategy to search a candidate DAG  $B$ , with a bounded tree-width constraint, within the subset of DAGs

$B$  such that  $\text{supp}(B) \subset \text{supp}(\Theta)$ . On the other hand, Ghoshal recovers the topological order of the causal graph by identifying and removing the terminal variables from the causal system; this sequential procedure requires updating (due to the dynamical nature of the *remaining graph*) the precision matrix estimator and has a complexity of  $O(d^3)$  when the precision matrix is sparse.

The proposed method ICID similar to [LB14, GH18], relies on the inverse covariance matrix  $\Theta$ , especially the sparsity pattern  $\text{supp}(\Theta)$ , but the inverse covariance information is used in a different way: we use the support graph  $\text{supp}(\Theta)$  as a source of subspace information for the matrix decomposition model (7).

When we choose the GraphicalLasso formulation [FHT07] (see (10)) for estimating the inverse covariance (line 1 of Algorithm 1), we recover the precision matrix associated with the MLE estimator  $B^*$  of GOLEM [NGZ20]. GOLEM estimates directly the causal graph adjacency matrix  $B^*$  from the same likelihood function: In fact, the objective function of (10) satisfies (ignoring the constant term  $-\frac{d}{2} \log(2\pi)$ )

$$\begin{aligned} \frac{1}{2}f(\Theta; X) &:= \frac{1}{2n} \text{tr}(X^T \Theta X) - \frac{1}{2} \log \det(\Theta) \\ &= \frac{1}{2n} \text{tr}((X - B^T X)^T \Omega^{-1} (X - B^T X)) + \frac{1}{2} \log \det(\Omega) - \log |\det(I - B^*)| \\ &= -\log p(B, \Omega; X), \end{aligned}$$

where  $\log p(B, \Omega; X)$  is the log-likelihood of  $(B, \Omega)$ , i.e., the objective function of GOLEM. The difference, however, is that the inverse covariance estimation is known to be a convex problem (over the cone  $\mathcal{S}_{++}^d$ ) and enjoys a much lower time complexity than the causal MLE within GOLEM. The overall time complexity of ICID (see Section 4.1) is also much lower than GOLEM.

## 5 Experiments

In this section, we examine the performance of the proposed method in causal structural learning and compare it with several baseline methods including GES [Chi02], DirectLiNGAM [SIS<sup>+</sup>11], NOTEARS[ZARX18], Ghoshal [GH18], and GOLEM [NGZ20]. First, we conduct experiments for causal structural learning on mid-sized random graphs. Then we evaluate the scalability and time efficiency of the proposed method in comparison with two NOTEARS and GOLEM in learning large causal graphs. We also test the proposed method (both ICID and the oracle version,  $\mathcal{O}$ -ICID) on a real-world protein dataset.

All structural learning methods are evaluated by the standard classification metrics (SHD, TPR, FDR and FPR) for (0-1) edge prediction of directed graphs. Details of these metrics are given in the supplementary material.

Results of all CPU-based methods are obtained on one single CPU of Intel(R) Xeon(R) Gold 5120 14 cores @ 2.2GHz and the results of GOLEM are obtained on a GPU of Tesla V100-PCIE-32GB.

Implementation details of the proposed method are given in Appendix A. The code is made available at <https://github.com/shuyu-d/icid-exp>.

**Random graphs and synthetic data.** The experiments on synthetic data are conducted with DAGs generated from two sets of random graphs: (i) Erdős–Rényi (ER) graphs and (ii) Scale-free (SF) [BA99] graphs, as characterized in Table 1.

Table 1: Features of different graph models.

|             | Parameter      | Degree distribution          |
|-------------|----------------|------------------------------|
| Erdős-Rényi | $p \in (0, 1)$ | Binomial $\mathcal{B}(d, p)$ |
| Scale-free  | $\gamma$       | $P(k) \propto k^{-\gamma}$   |

The generation of random DAGs from the two sets above is the same as in [ZARX18, NGZ20]. The naming of these graphs has a node degree specification, such as ‘ER1’, where the number indicates the average node degree of the graph. Specifically, for a given DAG  $\mathcal{G}^*$ , its weighted adjacency matrix  $B^*$  is generated by assigning weights to the nonzeros of  $\mathbb{B}(\mathcal{G}^*) \in \{0, 1\}^{d \times d}$  independently from the uniform distribution:  $B_{ij}^* \sim \text{Unif}([-2, -0.5] \cup [0.5, 2])$ , for  $(i, j) \in \text{supp}(\mathbb{B}(\mathcal{G}^*))$ . We generate observational data according to the linear SEM model (1), and store them in dataset  $X \in \mathbb{R}^{n \times d}$  where  $n$  is the number of samples. The additive noises of the linear SEM such that  $X = B^{*\text{T}}X + E$ , belong to either of the following models: (i) Gaussian noise (Gaussian):  $E \sim \mathcal{N}(0, \Omega)$  and (ii) Exponential noise (Exponential):  $E \sim \text{Exp}(\Omega)$ , where  $\Omega$  is a diagonal matrix of noise variances. Therefore, the dataset  $X$  belongs to one of the following categories  $\{\text{ER}k, \text{SF}k\} \times \{\text{Gaussian}, \text{Exponential}\}$  (where  $k$  is the aforementioned average node degree).

## 5.1 Structural learning performance

We conduct an experiment on data generated from linear SEMs described above. In this experiment, we test with ER $k$  graphs for  $k \in [0.2, 2]$  (including  $k = 1$  and 2) and SF $k$  for  $k \in \{1, 2\}$ , and set up the noise variances as  $\Omega = \sigma_N I$  for  $\sigma_N = 1$ . Note that the noise level is moderate (not too small) given that the amplitude of true edge weights  $|B_{ij}^*|$  is between  $[0.5, 2]$ .

For each type of SEMs, we use a dataset  $X \in \mathbb{R}^{n \times d}$  of  $n = 32d$  samples as the input data of the ICID method (Algorithm 1) and use a subset  $X'$  of  $n' = 10d$  samples for the baseline methods. The reason for testing ICID with more samples is purely practical, since for the statistical subproblem (inverse covariance estimation) of ICID, we use the basic empirical estimator (for line 1 Algorithm 1) that requires a sufficient number of samples, while with the baseline methods, we find that  $n = 32d$  is more than sufficient and increases the computational cost for most of them (except for Ghoshal, also based on inverse covariance estimation).

The learning performances of all methods are evaluated against the ground-truth adjacency matrix  $\mathbb{B}(\mathcal{G}^*)$  with standard structural learning metrics (SHD, TPR, FDR and FPR).

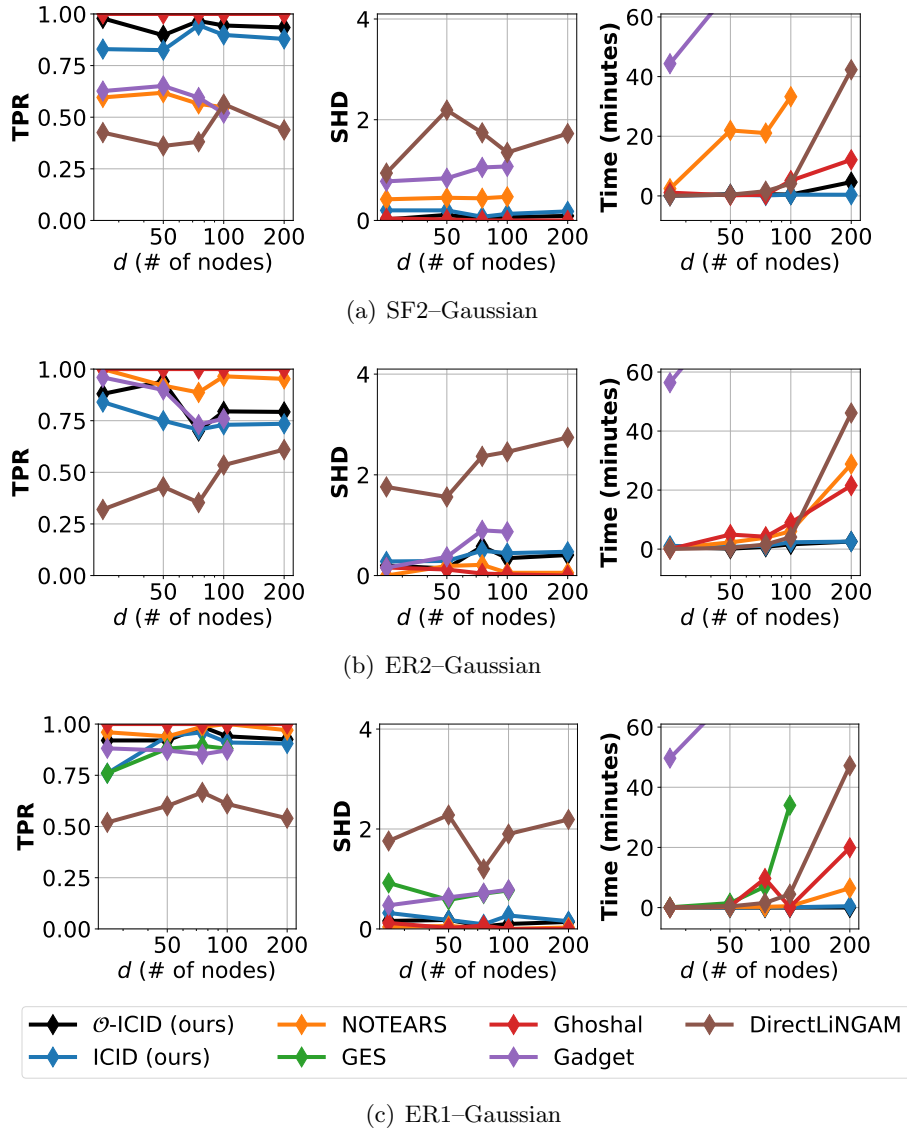


Figure 1: Structural learning results on linear SEM data with Gaussian noise, on ER1, ER2 and SF2 graphs. Number of nodes  $d \in \{25, 50, 75, 100, 200\}$ . The ‘SHD’ in the middle subplots denotes by abuse the normalized value:  $\text{SHD}/\|B^*\|_0$ .

The results are given in Figure 1. In particular, the learning accuracy of DirectLiNGAM in this experiment are not informative enough since DirectLiNGAM is designed for learning linear SEMs with non-Gaussian noises; DirectLiNGAM is still included for completeness of the benchmark of computation time (right column of Figure 1). We have the following observations:

- ICID and  $\mathcal{O}$ -ICID outperform all baseline methods in time efficiency: the speed-ups over Ghoshal in computation time range from around 10 times to 20 times, when  $d = 200$ , on all three types of graphs; and the speed-ups over NOTEARS are around 5 times on ER1 and around 25 times on ER2.
- In terms of learning accuracy (TPR and SHD), the proposed ICID performs similarly as the oracle ICID ( $\mathcal{O}$ -ICID), knowing that the number  $n$  of samples is sufficiently large for ICID. The two ICID methods, regrouped, give the second best solutions for ER1 and SF2, close to the best performing solutions of Ghoshal, and they give the third best solutions for ER2 after Ghoshal and NOTEARS.

Moreover, even though the graphs tested in this experiment are still small- or mid-sized, we already observe that the computation time of both ICID methods grow with  $d$  at a much slower rate than all other methods. This agrees with their much reduced theoretical time complexity ( $O(d^2)$  instead of  $O(d^3)$  or higher).

## 5.2 Scalability

We conduct experiments on high-dimensional data and compare the proposed method with NOTEARS and GOLEM. The random graph and data generation is as described in Section 5 and Section 5.1 but with the number of nodes set to larger values:  $d \in \{200, 400, \dots, 2 \cdot 10^3, 3 \cdot 10^3\}$ . While the proposed algorithm has a lower complexity and is capable of running on even larger graphs, we choose to scale the graphs up to  $d \leq 3 \cdot 10^3$  nodes to keep the total running time with the three methods manageable. Note that while ICID and NOTEARS run on CPU, the implementation of GOLEM leverages parallel computation for optimizing the MLE-based objective function and runs on a GPU. Nevertheless, it is interesting to compare their time efficiency in view of a large part of gradient-based optimization components in their respective designs.

Results are presented in Figure 2.

We observe that the computation time of both ICID methods increase with  $d$  with a much slower rate than GOLEM and NOTEARS: on ER1, the speedups over GOLEM are around 5 times at  $d = 2000$  and 10 times at  $d = 3000$ ; their speedups over NOTEARS are even greater when  $d \geq 1000$ . At the same time, the loss in learning accuracy of ICID compared to the state-of-the-art performances (which are almost 100% accurate for the sparse ER0.5 and ER1 graphs) of GOLEM and NOTEARS stay in a reasonable range, as we see that the TPRs are above 85%, and the normalized SHD within 20% in all tests.

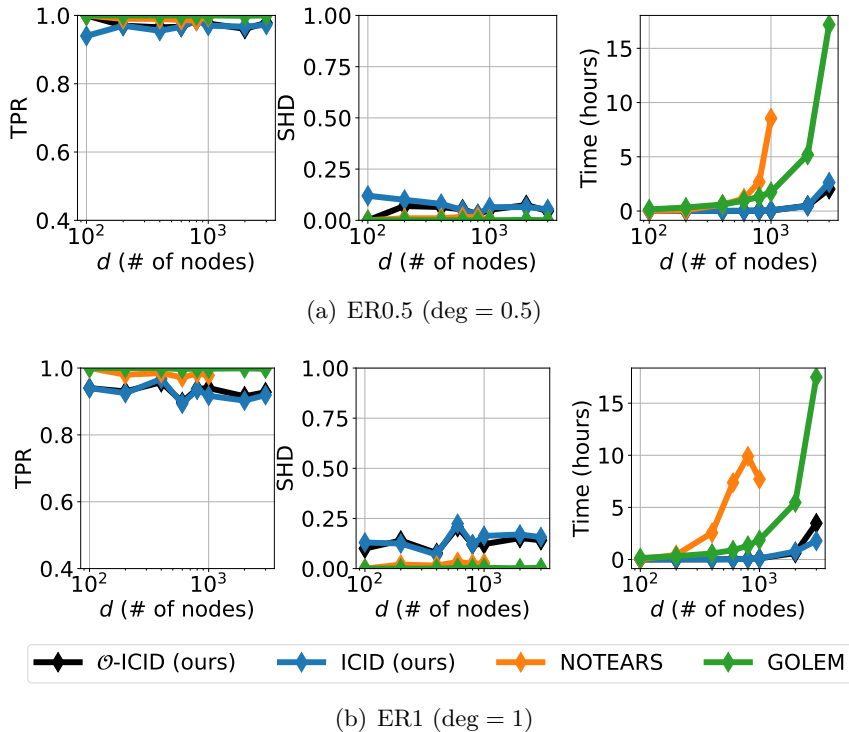


Figure 2: Structural learning results on linear SEM data with Gaussian noise, on ER0.5, ER1 graphs. Number of nodes  $d \in \{200, 400, \dots, 2000, 3000\}$ . The ‘SHD’ in the middle subplots denotes by abuse the normalized value:  $\text{SHD}/\|B^*\|_0$ .

### 5.3 Real data

We test the proposed method on a benchmark protein signaling dataset [SPP<sup>+</sup>05]. The dataset contains consists of  $n = 853$  observed expression signals of  $d = 11$  proteins with an expert-provided ground-truth graph. The true structure has 17 edges. We use all  $n = 853$  samples as input data of the proposed ICID and ICID-ideal algorithms. Results are presented in Table 2.

We observe that the average accuracy of ICID is similar to GOLEM (EV and NV version) with  $n = 100$  samples, which are less interesting than BCD-Nets (NV)’s results. When using all  $n \approx 800$  samples, however, ICID give solutions that are more informative than in the previous case. In particular, the oracle ICID,  $\mathcal{O}$ -ICID takes as input  $\Theta := (I - B^*)(I - B^*)^T$ —the precision matrix associated with the linear SEM and the ground-truth DAG  $B^*$ . We observe that  $\mathcal{O}$ -ICID gives solutions with an average SHD of 9.0, which outperforms by far the best scores (13.9 by Gadget and 14.7 by BCD Nets) reported in [CGE21, §5.2].

Table 2: Causal structure learning on the protein dataset [SPP<sup>+</sup>05]. The results of GOLEM and BCD-Nets are given by [CGE21].

|                            | $n$ | # Edges        | SHD            | Time (sec)      |
|----------------------------|-----|----------------|----------------|-----------------|
| BCD-Nets (EV)              | 100 | $11.3 \pm 1.2$ | $19.5 \pm 0.3$ | –               |
| BCD-Nets (NV)              | 100 | $9.2 \pm 2.0$  | $14.7 \pm 0.9$ | –               |
| GOLEM (EV)                 | 100 | $1.5 \pm 1.3$  | $18.5 \pm 1.3$ | –               |
| GOLEM (NV)                 | 100 | $1.5 \pm 1.3$  | $18.5 \pm 1.3$ | –               |
| ICID (ours)                | 100 | $11.6 \pm 3.7$ | $18.5 \pm 2.5$ | $3.92 \pm 4.29$ |
|                            | 853 | $5.7 \pm 2.7$  | $17.3 \pm 1.4$ | $1.74 \pm 0.44$ |
| $\mathcal{O}$ -ICID (ours) | NA  | $12.0 \pm 0.0$ | $9.0 \pm 0.7$  | $1.53 \pm 0.01$ |

## 6 Conclusion and Perspectives

The central claim of the paper is that the causal DAG discovery problem can be decomposed into a *statistical* and a *geometrical* part. The statistical part in the presented ICID consists of estimating the inverse covariance matrix  $\Theta$ , while the geometrical part consists of computing a support-preserving decomposition  $\Theta$  where the subspace information of  $B$  is implicitly restricted by the support-preserving constraint.

The main contribution of the paper is that the geometrical part of the causal DAG discovery problem is shown to be able to scale up to a number of variables  $d$  of a few thousands with significant speedups compared to the state-of-the-art methods. The proposed method leverages well-known results on the decomposition of chordal graphs, under the mild assumption that the inverse covariance matrix itself corresponds to a chordal graph or very close to one. Further work is concerned with establishing identifiability guarantees for the approach.

The extensive comparison with the state-of-the-art (DirectLiNGAM, NOTEARS, GOLEM and BCD-Net) shows the competence region of the ICID algorithm. It establishes that ICID computational runtime is lesser by an order of magnitude compared to GOLEM, and its limitations w.r.t. the known factors of difficulty of the problem: the sparsity of the sought DAG, its degree and the size of the available data (the number  $n$  of data samples divided par  $d$ ). At the moment, the main weakness in ICID is due to the estimation of the inverse covariance matrix: the current empirical estimator makes it necessary to consider sufficiently many samples ( $n = 32d$ ) in order to avoid degenerated results.

It is emphasized that these factors of difficulty are all related to the estimation of the inverse covariance matrix, that is, the *statistical* part of the ICID approach. Further work will focus on this aspect, leveraging data augmentation techniques and bootstrap, and exploiting the structure of the nnz pairs across the bootstrapped estimates, e.g. using supervised machine learning to learn to identify the true pairs from their estimates depending on the family of considered graphs, in the spirit of the Cause-Effect Pair Challenge [GSB19].

## A Implementation details

In this section, we present the implementation details of ICID (Algorithm 1–Algorithm 2). The oracle version,  $\mathcal{O}$ -ICID, corresponds to Algorithm 2 with an input inverse covariance  $\Theta$  obtained from oracles such as the matrix equation (2) for a ground-truth DAG  $B$  given.

### A.1 Inverse covariance estimation

The first part of ICID, line 1 in Algorithm 1, is to estimate the inverse covariance matrix given  $n$  data samples of  $\mathbf{X}$ . For this purpose, a basic, empirical inverse covariance estimator is computed as in Algorithm 3.

---

**Algorithm 3** Empirical inverse covariance estimator

---

**Input:** Data matrix  $X \in \mathbb{R}^{n \times d}$ , parameter  $\lambda_1 \in (0, 1)$

**Output:**  $\hat{\Theta}_{\lambda_1} \in \mathbb{R}^{d \times d}$

- 1: Compute empirical covariance and its inverse:

$$\hat{C} = \frac{1}{n}(X - \bar{X})^T(X - \bar{X}) \quad \text{and} \quad \hat{\Theta} = \hat{C}^\dagger, \quad (17)$$

where  $\hat{C}^\dagger$  denotes the pseudo-inverse of  $\hat{C}$ .

- 2: Element-wise thresholding on off-diagonal entries:

$$\begin{aligned} \text{diag}(\hat{\Theta}_{\lambda_1}) &:= \text{diag}(\hat{\Theta}), \\ (\hat{\Theta}_{\lambda_1})_{\text{off}} &:= \mathbb{H}(\hat{\Theta}_{\text{off}}, \lambda_1 \|\hat{\Theta}_{\text{off}}\|_{\max}), \end{aligned} \quad (18)$$

where  $\mathbb{H}$  is defined as

$$\mathbb{H}(y, \tau) = \begin{cases} y & \text{if } |y| \geq \tau \\ 0 & \text{otherwise.} \end{cases}$$


---

In the computation of (17), the pseudo-inverse coincides with the inverse of  $\hat{C}$  when  $\hat{C}$  is positive definite (e.g., when the number  $n$  of samples is sufficiently large). In (18), the subscript ‘off’ indicates the following filtering operation

$$\Theta_{\text{off}} = \{\Theta_{ij} : i \neq j\}$$

where the indices of the remaining (off-diagonal) entries are preserved.

### A.2 Independence-based Decomposition (Algorithm 2)

An implementation of Algorithm 2 is given in Algorithm 4.

The operator for graph support projection in Algorithm 4, line 10 is as follows.



---

**Algorithm 4** (Algorithm 2 in detail): Independence-based Decomposition

---

**Input:** Inverse covariance matrix  $\Theta \in \mathbb{R}^{d \times d}$ ,  $\lambda'_1 > 0$ , function  $f$  (13b),  $\alpha_0 > 0$ ,  $\gamma \in (0, 1)$ ,  $\beta = \frac{1}{2}$ , tolerance  $\epsilon, \epsilon', \rho \in (0, 1)$ , low-rank parameter  $r$ .

**Output:**  $\tilde{B}_{t+1}$

1: Initialize:  $W_0 = \mathbf{0}_{d \times d}$ , set  $Y_0 = W_0$ .

2: **for**  $s = 1, 2, \dots$  **do**

3: Backtracking: find smallest integer  $k_s \geq 0$  such that, for  $\tilde{\eta}_s := \alpha_0 \beta^{k_s}$ ,

$$f(\tilde{W}) - f(Y_{s-1}) \leq -\gamma \tilde{\eta}_s \|\text{grad}_{\mathcal{C}_\Theta} f(Y_{s-1})\|^2,$$

where

$$\tilde{W} = \text{prox}_{\tilde{\eta}_s \lambda'_1 \ell_1} (Y_{s-1} - \tilde{\eta}_s \text{grad}_{\mathcal{C}_\Theta} f(Y_{s-1})).$$

# see (21)-(22)

4: Update FISTA iterates:

$$W_s = \tilde{W} \quad \text{and} \quad Y_s = W_s + \frac{s-1}{s+2} (W_s - W_{s-1}).$$

5: Stop if  $\|\Delta(W_s)\|_F \leq \epsilon$ :

# see (23)

return  $B_0 := W_s$  (13)

6: **end for**

7: **Compute proximal DAGs:** Initialize  $\gamma_2 = 1$  and rank parameter by  $r$  (for the search space  $\mathbb{R}^{d \times r} \times \mathbb{R}^{d \times r}$ )

$\tilde{B}_0 := B_0$ .

8: **for**  $t = 0, 1, \dots$  **do**

9: Interpolate:  $B_{t+1} = (1 - \rho)B_0 + \rho \tilde{B}_t$

10: Compute  $\tilde{B}_{t+1} := \text{LoRAM-AGD}(\gamma_2 g + h, S)$  with

- Update of support graph  $S := \text{supp}(B_{t+1})$
- Update of  $g(\cdot; B_{t+1})$  and  $h$  for gradient oracles of LoRAM:

$$g(U, V) \leftarrow g \circ \bar{P}_S(U, V) \quad \# \text{ see (12a)}$$

$$h(U, V) \leftarrow h \circ \bar{P}_S(U, V) \quad \# \text{ see (12b)}$$

where  $\bar{P}_S(U, V) := P_S(UV^T)$ .

# see Definition 7

11: Increment  $(1/\gamma_2)$ :

$$\gamma_2 \leftarrow \gamma_2/5 \quad \text{if } h(\tilde{B}_{t+1}) > h(\tilde{B}_t). \quad (19)$$

12: Stop if  $h(\tilde{B}_{t+1}) \leq \epsilon'$

13: **end for**

---

**Definition 7.** Given  $S \in \mathbb{R}^{d \times d}$ , the projection onto the support graph  $\text{supp}(S)$  is denoted and defined as  $P_S : \mathbb{R}^{d \times d} \rightarrow \mathbb{R}^{d \times d}$  such that

$$(P_S(Z))_{ij} = \begin{cases} Z_{ij} & \text{if } (i, j) \in \text{supp}(S) \\ 0 & \text{otherwise.} \end{cases}$$

**Decomposition (13).** The computation of decomposition (13) is given in Algorithm 4, lines 1–6. The FISTA [BT09] is applied to solving (13) in view of the  $\ell_1$  norm penalty term.

The support constraint of (13), along with the prior knowledge that  $\text{diag}(B) = \mathbf{0}$  (since a candidate adjacency matrix  $B$  does not admit any self-cycle), imposes that the maximal search space of the problem is the following set

$$\mathcal{C}_\Theta := \{B \in \mathbb{R}^{d \times d} : B_{ij} = 0 \quad \forall i = j \text{ or } (i, j) \notin \text{supp}(\Theta)\}, \quad (20)$$

which is a (linear) subspace of  $\mathbb{R}^{d \times d}$  with dimension  $(\|\Theta\|_0 - d)$ . This means that the constraint of (13) can be satisfied using subspace projection straightforwardly.

Denote the smooth part of the objective function of (13) by

$$f(B) := \frac{1}{2} \|\Theta - \phi(B)\|_{\mathbb{F}}^2. \quad (13b)$$

The gradient  $\nabla f(B)$  is given in Proposition 6. From definition (20), it follows that the gradient of  $f$  restricted to subspace  $\mathcal{C}_\Theta$  (20), denoted as  $\text{grad}_{\mathcal{C}_\Theta} f$ , is

$$\text{grad}_{\mathcal{C}_\Theta} f(B) = P_{\mathcal{C}_\Theta}(\nabla f(B)), \quad (21)$$

where  $P_{\mathcal{C}_\Theta} : \mathbb{R}^{d \times d} \rightarrow \mathcal{C}_\Theta$  is the projection (Definition 7) onto the support of  $\Theta_{\text{off}}$ .

On the other hand, the proximal operator associated with the  $\ell_1$  term of (13) is

$$\text{prox}_{\lambda \ell_1}(Z) = \begin{cases} \text{sign}(Z_{ij})(|Z_{ij}| - \eta) & \text{if } |Z_{ij}| \geq \lambda \\ 0 & \text{otherwise.} \end{cases} \quad (22)$$

In Algorithm 4, line 5, the stopping criterion is defined with respect to  $\ell_1$ -subdifferential optimality. Hence  $\Delta(B) \in \mathbb{R}^{d \times d}$  is as follows:

$$\begin{aligned} (\Delta(B))_{ij} &= -(\text{grad}_{\mathcal{C}_\Theta} f(B))_{ij} - \lambda'_1 \text{sign}(B_{ij}) \text{ if } B_{ij} \neq 0, \\ (\Delta(B))_{ij} &= |(\text{grad}_{\mathcal{C}_\Theta} f(B))_{ij}| - \lambda'_1 \text{ if } B_{ij} = 0 \text{ and} \\ &\quad |(\text{grad}_{\mathcal{C}_\Theta} f(B))_{ij}| \geq \lambda'_1, \\ (\Delta(B))_{ij} &= 0 \text{ otherwise.} \end{aligned} \quad (23)$$

*Remark 8 (Alternatives).* Decomposition (13) can be computed by standard solvers for matrix decomposition, with a light adaptation to the  $\ell_1$  penalty term.  $\square$

**Proximal DAGs** (14)–(15). The computation of (14)–(15) is given in lines 7–13 of Algorithm 4. In view of reducing the complexity due to the exponential trace-based function  $h$  in (15), the low-rank method LoRAM-AGD of [DS22] is used.

More precisely, proximal mapping (15) is defined as a solution to

$$\min_{B \in \mathbb{R}^{d \times d}} h(B) + \gamma_2 \underbrace{\|B - c_0 B_{t+1}\|_{\mathbb{F}}^2}_{g(B; B_{t+1})}, \quad (12a)$$

where  $h$  is the exponential trace-based function

$$h(B) = \text{tr}(\exp(|B|)) \quad (12b)$$

with the absolute value operation  $|\cdot|$  applied to  $B$  element-wisely. Due to the exponential trace in  $h$  [ZARX18], problem (12) is nonconvex. We resort to the search of one proximal point (15) satisfying sufficient decrease in  $h$ . For this purpose, the increment rule (19), an ad-hoc adaptation of the AMA (alternating minimization algorithm) for optimizing the Lagrangian of an equality constrained optimization, is used.

### A.3 Parameters of ICID

The parameters of ICID (Algorithm 1), from Algorithm 3–Algorithm 4, are summarized in the following list, along with the values chosen.

- Parameter  $\lambda_1$  in Algorithm 3: see Appendix B.1.
- Parameter  $\lambda'_1$  for (13) is chosen by grid search on 5 equidistant points in  $[4.10^{-2}, 8.10^{-2}]$ .  $\lambda'_1$  plays a similar role as the  $\lambda_1 \ell_1$ -penalty terms of NOTEARS and GOLEM, but it is set to smaller values than for the latter two methods, given that there are final computation of proximal DAGs (15) following (13).
- Line search parameters in Algorithm 4:  $\alpha_0 = \lambda_{\max}(\Theta)$  (maximal eigenvalue),  $\gamma = \frac{1}{2}$ .
- Tolerance parameters in Algorithm 4:  $\epsilon = 10^{-4}$ ,  $\epsilon' = 10^{-12}$ .
- Parameters for (15) of Algorithm 4:  $c_0 = 10^{-2}$ , and low-rank parameter  $r = 25$ , hard threshold parameter  $\epsilon_r = 2.10^{-1}$ . See Remark 9.
- Parameter for the interpolation step (14):  $\rho = 0.7$ .
- Parameter  $\gamma_2 = 1$ , with incremental rule (19).

All values given above are mostly related to sufficient decrease and optimality conditions. They are data-independent, assuming, without loss of generality, that the scale of the inverse covariance is such that  $\|\Theta_{\text{off}}\|_{\max} \asymp 1$ .

*Remark 9.* In particular: (i) constant  $c_0$  is used in [DS22] to rescale the input graph for numerical stability. The reverse rescaling of the solution, by  $c_0^{-1}$ , is implicitly included by abuse of notation within the end of the proximal mapping computation. (ii) The rank parameter  $r = 25$  is observed to be pertinent in all experiments with  $25 \leq d \leq 3 \cdot 10^3$ ; This choice holds empirically for  $d \asymp 10^3$  mainly due to the sparsity of graphs tested in the experiments.  $\square$

## B Experiments

### B.1 Evaluation Metrics

Below are the four common graph metrics (see, e.g., [ZARX18, E.2]): (1) True positive rate (TPR), (2) False discovery rate (FDR), (3) False positive rate (FPR), and (4) Structural Hamming distance (SHD), which are defined as

1.  $\text{TPR} = \text{TP}/\text{T}$  (*higher is better*),
2.  $\text{FDR} = (\text{R} + \text{FP})/\text{P}$  (*lower is better*),
3.  $\text{FPR} = (\text{R} + \text{FP})/\text{F}$  (*lower is better*),
4.  $\text{SHD} = \text{E} + \text{M} + \text{R}$  (*lower is better*).

More precisely, SHD is the (minimal) total number of edge additions (E), deletions (M), and reversals (R) needed to convert an estimated DAG into a true DAG. Since a pair of directed graphs are compared, a distinction between True Positives (TP) and Reversed edges (R) is needed: the former is estimated with correct direction whereas the latter is not. Likewise, a False Positive (FP) is an edge that is not in the undirected skeleton of the true graph. In addition, Positive (P) is the set of estimated edges, True (T) is the set of true edges, False (F) is the set of non-edges in the ground truth graph. Finally, let (E) be the extra edges from the skeleton, (M) be the missing edges from the skeleton.

*Remark 10.* In Figure 1–Figure 2, the SHDs with respect to the ground-truth DAG  $B^*$  of each test, reported on Y-axis, are normalized by constant  $\text{nnz}(B^*)$ . In Table 2, on the other hand, the SHDs are original, non-normalized values.  $\square$

### B.2 Selection of $\lambda_1$ for inverse covariance

We use grid search for selecting values of  $\lambda_1$  for the empirical inverse covariance estimator (Algorithm 3). Note that the total time for selecting the value of  $\lambda_1$  using Algorithm 3 is counted as the computation time for the first part, Algorithm 1, line 1, of ICID in all benchmarks of Section 5.

We start by estimating the grid search area of  $\lambda_1$ , based on observational data on ER graphs with  $200 \leq d \leq 2 \cdot 10^3$  nodes. The same methodology applies to SF graphs.

Given that most desired causal structures have an average degree  $1 \leq k \leq 4$ , the target sparsity of  $\widehat{\Theta}_{\lambda_1}$  by Algorithm 3 is bounded by  $\bar{\rho}_k = \max(\frac{k}{d}) \approx 2.0\%$  for graphs with  $d \geq 200$  nodes. This gives us an approximate target percentile of around 98%, i.e., top 2% edges in terms of absolute weight of  $\widehat{\Theta}_{\text{off}}$ . In other words, the maximal value  $\lambda_1^{\max}$  of the grid search area is set as

$$\lambda_1^{\max} := \frac{|\widehat{\Theta}_{\text{off}}(\tau_{98})|}{\|\widehat{\Theta}_{\text{off}}\|_{\max}},$$

where  $\tau_{98}$  refers to the index of the 98-th percentile in  $\{|\widehat{\Theta}_{\text{off}}|\}$ . For the experiments with ER2 graphs in Section 5, the estimated  $\lambda_1^{\max}$  is  $6.10^{-1}$ . Hence, the search grid of  $\lambda_1$  is set up as  $n_{I_1} = 20$  equidistant values on  $I_1 = [10^{-2}, 6.10^{-1}]$ .

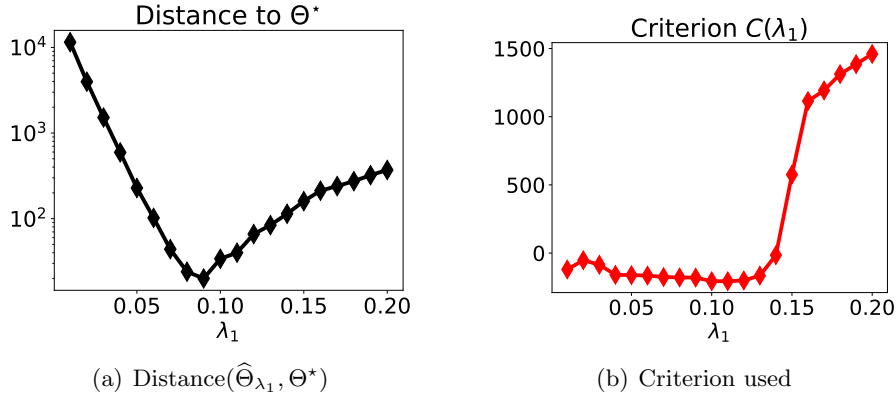


Figure 3: Grid search of  $\lambda_1$  with Algorithm 3 based on criterion  $C(\lambda_1)$  (24). Data  $X$  is from linear SEM with Gaussian noise, on ER2 graph with  $d = 200$  nodes.

The selection criterion, similar to GraphicalLasso, is defined as

$$C(\lambda_1) := \text{tr}(\widehat{C}\widehat{\Theta}_{\lambda_1}) - \log \det(\widetilde{\Theta}_{\lambda_1}), \quad (24)$$

where  $\widetilde{\Theta}_{\lambda_1} = \widehat{\Theta}_{\lambda_1} + \frac{9}{10} \text{diag}(\widehat{\Theta}_{\lambda_1})$  is used in the log det-evaluation for an enhanced positive definiteness in all cases.

Figure 3 shows the criterion values compared to the Hamming distances with the oracle precision matrix  $\Theta^* := \phi(B^*)$ . We observe that the selection criterion with  $\arg \min_{I_1} C(\lambda_1)$  gives an answer that is rather close to the optimal value in terms of distance of  $\widehat{\Theta}_{\lambda_1}$  to the oracle precision matrix  $\Theta^*$ .

### B.3 Empirical convergence behavior of ICID

Figure 4 presents iteration histories of ICID in terms of (i) the optimality criterion  $\|\Delta(B_0)\|_F$  (23) during the computation of (13), and (ii) the DAG constraint violation measure  $h(B_0)$  and  $h(\widehat{B}_t)$  for all  $t$ .

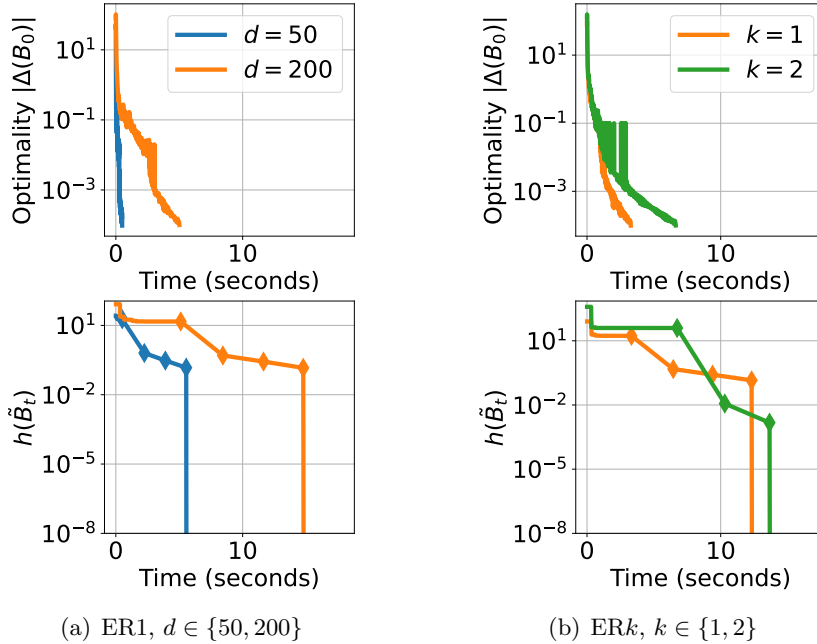


Figure 4: Iteration history of ICID. (a): ER1 graphs with  $d \in \{50, 200\}$ , and (b): ER $k$  graphs with  $d = 200$  nodes and  $k \in \{1, 2\}$ .

In both cases (a)–(b) shown in Figure 4, the final proximal DAGs (15) are no longer visible on the log-scale plot since they attain exactly zero in function value of  $h$ . These sharp decreases in  $h$  at the end of iterations are due to the hard thresholding operation within the computation of proximal DAGs (15); since the iterates  $\{B_t\}_{t \geq 0}$  are already at least  $\epsilon$ -optimal (in terms of  $\|\Delta(B)\|_F$  (23)) after decomposition (13), it is highly probable that the proximal DAGs (15) hit an exact DAG in a few iterations.

## References

- [ABGLP19] Martin Arjovsky, Léon Bottou, Ishaan Gulrajani, and David Lopez-Paz. Invariant risk minimization. *arXiv preprint arXiv:1907.02893*, 2019.
- [BA99] Albert-László Barabási and Réka Albert. Emergence of scaling in random networks. *science*, 286(5439):509–512, 1999.
- [BEGd08] Onureena Banerjee, Laurent El Ghaoui, and Alexandre d’Aspremont. Model selection through sparse maximum likelihood estimation for multivariate gaussian or binary data. *The Journal of Machine Learning Research*, 9:485–516, 2008.

- [BT09] Amir Beck and Marc Teboulle. A fast iterative shrinkage-thresholding algorithm for linear inverse problems. *SIAM journal on imaging sciences*, 2(1):183–202, 2009.
- [CGE21] Chris Cundy, Aditya Grover, and Stefano Ermon. BCD Nets: Scalable variational approaches for Bayesian causal discovery. In *Advances in Neural Information Processing Systems*, 2021. URL: <https://openreview.net/forum?id=gbtDcLzwKUb>.
- [Chi96] David Maxwell Chickering. Learning Bayesian networks is NP-complete. In *Learning from data*, pages 121–130. Springer, 1996.
- [Chi02] David Maxwell Chickering. Optimal structure identification with greedy search. *Journal of machine learning research*, 3(Nov):507–554, 2002.
- [DGE<sup>+</sup>22] Tristan Deleu, António Góis, Chris Emezue, Mansi Rankawat, Simon Lacoste-Julien, Stefan Bauer, and Yoshua Bengio. Bayesian structure learning with generative flow networks. *arXiv preprint arXiv:2202.13903*, 2022. URL: <https://arxiv.org/abs/2202.13903>, doi:10.48550/arxiv.2202.13903.
- [DS22] Shuyu Dong and Michèle Sebag. From graphs to DAGs: a low-complexity model and a scalable algorithm, 2022. URL: <https://arxiv.org/abs/2204.04644>.
- [FG65] Delbert Fulkerson and Oliver Gross. Incidence matrices and interval graphs. *Pacific journal of mathematics*, 15(3):835–855, 1965.
- [FHT07] Jerome Friedman, Trevor Hastie, and Robert Tibshirani. Sparse inverse covariance estimation with the graphical lasso. 2007. URL: <http://statweb.stanford.edu/~tibs/ftp/graph.pdf>.
- [FZS18] Salar Fattahi, Richard Y Zhang, and Somayeh Sojoudi. Sparse inverse covariance estimation for chordal structures. In *2018 European Control Conference (ECC)*, pages 837–844. IEEE, 2018.
- [FZZ<sup>+</sup>20] Zhuangyan Fang, Shengyu Zhu, Jiji Zhang, Yue Liu, Zhitang Chen, and Yangbo He. Low rank directed acyclic graphs and causal structure learning. *arXiv preprint arXiv:2006.05691*, 2020.
- [GH18] Asish Ghoshal and Jean Honorio. Learning linear structural equation models in polynomial time and sample complexity. In *International Conference on Artificial Intelligence and Statistics*, pages 1466–1475. PMLR, 2018.
- [GSB19] Isabelle Guyon, Alexander R. Statnikov, and Berna Bakir Batu, editors. *Cause Effect Pairs in Machine Learning*. Springer, 2019. doi:10.1007/978-3-030-21810-2.

- [KB07] Markus Kalisch and Peter Bühlman. Estimating high-dimensional directed acyclic graphs with the pc-algorithm. *Journal of Machine Learning Research*, 8(3), 2007.
- [KGG<sup>+</sup>18] Diviyani Kalainathan, Olivier Goudet, Isabelle Guyon, David Lopez-Paz, and Michèle Sebag. Structural agnostic modeling: Adversarial learning of causal graphs. *arXiv preprint arXiv:1803.04929*, 2018.
- [LB14] Po-Ling Loh and Peter Bühlmann. High-dimensional learning of linear causal networks via inverse covariance estimation. *The Journal of Machine Learning Research*, 15(1):3065–3105, 2014.
- [NGZ20] Ignavier Ng, AmirEmad Ghassami, and Kun Zhang. On the role of sparsity and DAG constraints for learning linear DAGs. *Advances in Neural Information Processing Systems*, 33:17943–17954, 2020.
- [NZZZ21] Ignavier Ng, Yujia Zheng, Jiji Zhang, and Kun Zhang. Reliable causal discovery with improved exact search and weaker assumptions. *Advances in Neural Information Processing Systems*, 34:20308–20320, 2021.
- [PBM16] Jonas Peters, Peter Bühlmann, and Nicolai Meinshausen. Causal inference by using invariant prediction: identification and confidence intervals. *Journal of the Royal Statistical Society. Series B (Statistical Methodology)*, pages 947–1012, 2016.
- [Pea00] Judea Pearl. *Causality: Models, Reasoning and Inference*. Cambridge University Press, 2000.
- [PJS17] Jonas Peters, Dominik Janzing, and Bernhard Schölkopf. *Elements of causal inference: foundations and learning algorithms*. The MIT Press, 2017.
- [PPS89] Vern I Paulsen, Stephen C Power, and Roger R Smith. Schur products and matrix completions. *Journal of functional analysis*, 85(1):151–178, 1989.
- [SG21] Axel Sauer and Andreas Geiger. Counterfactual generative networks. In *International Conference on Learning Representations (ICLR)*, 2021.
- [SHHK06] Shohei Shimizu, Patrik O Hoyer, Aapo Hyvärinen, and Antti Kerminen. A linear non-Gaussian acyclic model for causal discovery. *Journal of Machine Learning Research*, 7(10), 2006.
- [SIS<sup>+</sup>11] Shohei Shimizu, Takanori Inazumi, Yasuhiro Sogawa, Aapo Hyvärinen, Yoshinobu Kawahara, Takashi Washio, Patrik O Hoyer, and Kenneth Bollen. DirectLINGAM: A direct method for learning a linear non-Gaussian structural equation model. *The Journal of Machine Learning Research*, 12:1225–1248, 2011.



- [SPP<sup>+</sup>05] Karen Sachs, Omar Perez, Dana Pe’er, Douglas A Lauffenburger, and Garry P Nolan. Causal protein-signaling networks derived from multiparameter single-cell data. *Science*, 308(5721):523–529, 2005.
- [TKL<sup>+</sup>21] Stratis Tsirtsis, Amir-Hossein Karimi, Ana Lucic, Manuel Gomez-Rodriguez, Isabel Valera, and Hima Lakkaraju. ICML workshop on algorithmic recourse. 2021.
- [VHPK20] Jussi Viinikka, Antti Hyttinen, Johan Pensar, and Mikko Koivisto. Towards scalable Bayesian learning of causal DAGs. *Advances in Neural Information Processing Systems*, 33:6584–6594, 2020.
- [WJ06] Martin J Wainwright and Michael I Jordan. Log-determinant relaxation for approximate inference in discrete markov random fields. *IEEE transactions on signal processing*, 54(6):2099–2109, 2006.
- [WLR06] Martin J Wainwright, John Lafferty, and Pradeep Ravikumar. High-dimensional graphical model selection using  $\ell_1$ -regularized logistic regression. *Advances in neural information processing systems*, 19, 2006.
- [YCGY19] Yue Yu, Jie Chen, Tian Gao, and Mo Yu. DAG-GNN: DAG structure learning with graph neural networks. In *International Conference on Machine Learning*, pages 7154–7163. PMLR, 2019.
- [ZARX18] Xun Zheng, Bryon Aragam, Pradeep K Ravikumar, and Eric P Xing. DAGs with NO TEARS: Continuous optimization for structure learning. In *Advances in Neural Information Processing Systems*, volume 31, 2018. URL: <https://proceedings.neurips.cc/paper/2018/file/e347c51419ffb23ca3fd5050202f9c3d-Paper.pdf>.
- [ZDA<sup>+</sup>20] Xun Zheng, Chen Dan, Bryon Aragam, Pradeep Ravikumar, and Eric Xing. Learning sparse nonparametric dags. In *International Conference on Artificial Intelligence and Statistics*, pages 3414–3425. PMLR, 2020.